ICAS 2020 SHANG HAI
International Council of the Aeronautical Sciences
32nd Congress of the International Council of the Aeronautical Sciences
September 6-10, 2021
Pudong Shangri-La, Shanghai, China

Conceptual Design of Silent Electric Commuter Aircraft

Philip Wassink[1], Georgi Atanasov[1], Christian Hesse[1], Benjamin Fröhler[1]

[1] German Aerospace Center (DLR), Institute of System Architectures in Aeronautics, Hamburg

Abstract

Two hybrid-electric 19-seater air vehicle concepts with a focus on noise reduction are designed and evaluated on a conceptual level. The objective is a significant noise reduction compared to a conventional reference aircraft. Short take-off and landing, mixed passenger and cargo transport capability with operations in the low speed domain are identified as suitable aircraft characteristics that could make a viable business case for hybrid-electric commuter aircraft. A parallel and a serial hybrid-electric propulsion architecture are investigated. The resulting aircraft designs are compared against a conventional baseline aircraft that uses state-of-the-art technology. The timeframe of the year of entry into service is set to 2030 in order to match the technology level of next-generation lithium batteries. The results indicate that the serial-hybrid electric architecture has the potential to cut the perceived take-off noise emissions in half and perform better in terms of energy efficiency compared to the parallel-hybrid architecture. Both aircraft designs are shown to reduce the block energy demand on a 200 km sector by more than 70 % compared to the conventional baseline aircraft.

Keywords: conceptual aircraft design, electric aircraft, commuter aircraft, low-noise design

1. Introduction

The European Union has set a goal that by 2050, 90% of its citizens will be able to travel any distance within the continent from door to door in less than four hours [1]. Local, environmentally friendly air travel might aid in this goal. With improving lithium-battery technology, there is a potential for commuter class aircraft to serve short-haul connections between regional city hubs and remote locations where there is insufficient infrastructure. The short-haul transportation market has been studied in recent years. According to the findings of Paul et. al. [2] and Atanasov et. al. [3], in the year 2018 approximately 56 % of the civil worldwide 19-seater aircraft departures served routes of up to 200 km. Furthermore, CO2 emissions of the global 19-seater fleet could be cut by 45 % by replacing the fleet with an energy efficient hybrid-electric aircraft design that can achieve a full-electric range of 200 km. New business models like on-demand air-taxi services could revive the short-haul market and have the potential to save passengers minimum 40 minutes between relevant German city pairs [2]. Salucci et. al. [4] conducted an Italy based network study for an inter-city airliner service with origin destination pairs of up to 600 km distances between aerodromes with minimum runway lengths of 600 m. Thereafter, it was estimated that about 97 % of the total passenger demand was served with a stage length of 400 km between aerodromes with minimum runway lengths of 600 m. Reducing the noise and chemical emissions during ground handling through novel propulsion systems offers potential for aircraft operations at smaller airfields [4]. The subject of the present work is the derivation of aircraft designs suitable for the outlined potentials. It is a follow up on research activities from Atanasov et. al. [3] with a general focus laid on low-noise conceptual design. The market potential is then assessed based on origin destination pairs in a German network in a separate work by Papantoni et. al. [5].

The first part of the paper is a brief description of the overall aircraft design process. Then, the major design characteristics suitable for electric commuter aircraft are derived. Following that, the reference aircraft selected for the study is introduced. The subsequent section explains two investigated hybrid-electric architectures and the assumptions underlying the modelling of the electrical power devices. Further, various aspects of the aircraft design including noise reduction strategies are discussed.

Consequently, several parameters influencing the noise level of the aircraft are varied and final designs for each hybrid-electric architecture are selected. Both designs are afterwards compared to a conventional baseline aircraft with regard to energy efficiency and payload range capability. Finally, a conclusion on the differences between the two architectures and the potential of a silent electric commuter aircraft is drawn.

2. Aircraft Design Environment

The aircraft modelled in this paper are generated via the DLR inhouse software *openAD*. The Level 0 design tool has been introduced in detail by Woehler et. al. [6] and works with the Common Parametric Aircraft Configuration Schema (CPACS) [7]. The aircraft mission is calculated via a Level 1 mission performance tool that works with engine and aero performance decks. The trajectories for take-off and landing are computed via a Level 1 low-speed performance tool which was introduced by Froehler et. al. [8]. The modelling approach of the engine performance deck can be deduced from [8] as well. The aircraft noise according to the ICAO certification metric is estimated via a fast and simplified method for evaluating propeller aircraft, which was developed in [8]. All tools communicate through the CPACS interface, which allows rapid and automated aircraft design workflows. The present work represents a case study for the application of the newly acquired inhouse low-speed performance and noise assessment capabilities.

3. Silent Electric Commuter Design

3.1 Design for a Successful Business Case

According to the data presented by Paul et. al. [2], the market of civil 19-seater aircraft in 2018 was mainly split between six designs, see Table 1. As of 2021, three 19-seater aircraft remain in production [2]. Those are the Viking DHC-6, the L-410 and the Do228NG. There is also one newly developed aircraft, the Cessna SkyCourier, which is in its certification phase [9]. All four share the same operational domain of lower to medium speeds with unpressurized cabins with the ability to transport cargo.

Table 1: Market share of active 19-seater fleet [2]

Aircraft	Market Share [%]	Domain
DHC-6	24	Low-speed, Mixed Passenger & Utility
Beech 1900	23	High-speed, Airliner
Merlin IV/Metro	15	High-speed, Airliner
L-410	12	Low- to Medium-speed, Mixed Passenger & Utility
Jetstream 31	8	High-speed, Airliner
Do228	7	Medium-speed, Mixed Passenger & Utility

Since high-speed, high-performance commuter airliners are no longer produced, the needs of the commuter market seem to be best served by slower aircraft designs. This could be the targeted sector of a new battery-electric design, which is synergetic with the inherent capabilities of battery-electric aircraft due to their limited range. Lower speeds on short-haul flights allow operating the aircraft with optimal aerodynamic efficiency, thus maximizing the achievable electric range, which improves the competitiveness of battery-electric aircraft. Many of the existing low-speed commuter aircraft employ unpressurized, flexible cabin designs for passenger and cargo transport. Furthermore, most of these aircraft offer short take-off and landing capabilities (STOL). The study for an Italian network showed that runway lengths of minimum 600 m could provide about 60 % greater market potential for a commuter aircraft than runway lengths of minimum 1000 m independent of cruise speed [4]. Therefore, it is plausible to target STOL capabilities for battery-electric aircraft as well. As was mentioned before, more than half of the flights in 2018 were operated in the range of up to 200 km. Such short distances can be operated electrically, offering significant fuel and energy reduction potential. Additional gas turbines can be incorporated in the propulsion architecture to function as range extenders for increasing the operational flexibility of the design. A further synergy of such a propulsion chain is that the required energy for the mandatory reserve mission could be carried in the form of kerosene, allowing the full utilization of the battery for the main mission, similar to the concept presented by Atanasov et. al. [3].

The focus of the present work is to derive two aircraft designs that fulfill the outlined potential. Each proposed concept is also evaluated in terms of its potential for noise reduction. The only fixed top-level aircraft requirements for the designs is the STOL capability (take-off field lengths below 610 m) and the maximum cruise speed which is 230 KTAS. The aircraft range is a result dependent on the battery sizing strategy and not a requirement.

3.2 Reference Aircraft

All studies in the present work are based on extrapolations from a reference aircraft model that represents the Do228NG. The Do228NG is a twin-turboprop aircraft with STOL capabilities, flexible passenger/cargo cabin layout, an unpressurized fuselage and aluminum alloy airframe structure. The pilot operating handbook [10] together with a technical brochure [11] provided sufficient information for the validation of the conceptual model. A short summary on the key aircraft characteristics is given in Table 2. The assumptions for destination alternate distance is based on recommendations from [12] and the values for holding and contingency fuel are retrieved from regulations for commercial flight from [13]. The STOL and utility character of the Do228NG make it an ideal point of reference for the present study. A three view of the reference aircraft is given in Figure 1.

Table 2: Mass breakdown, performance and mission data of reference aircraft.

Parameter	Value	Unit	Parameter	Value	Unit
Payload			**Performance**		
Max. Passenger	19	-	Max. cruise Mach number	0.36	-
Max. Payload	2040	kg	Standard Payload (SPP)	1767	kg
Mass breakdown			Design range	688	km
Structure	1795	kg	**Engine**		
Propulsion	700	kg	Shaft power	580	kW
Systems	660	kg	Prop diameter	2.5	m
Furnishings	270	kg	Prop max. speed	1591	rpm
Operator items	475	kg	Prop max. tip Mach number	0.62	-
OEM	3900	kg	**Reserves**		
MZFM	5940	kg	Destination alternate distance	100	nm
MLM	6100	kg	Holding duration	30	min
MTOM	6400	kg	Contingency fuel (% trip fuel)	5	%

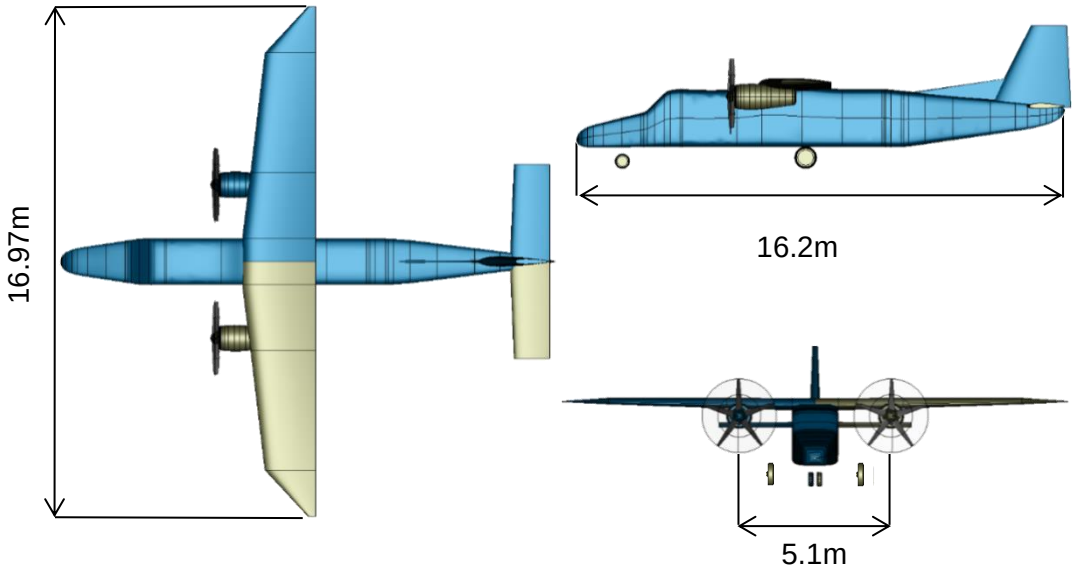

Figure 1: Three view of reference aircraft

3.3 Baseline Aircraft and Technology Assumptions

The baseline aircraft represents an evolutionary development of the reference aircraft with improved technology for airframe structures and conventional turboprop engines. This aircraft model provides a fair comparison of the unconventional silent commuter design with a conventional aircraft based on state-of-the-art technologies. The changes and improvements of the baseline aircraft relative to the reference aircraft are listed in Table 3. The hybrid-electric designs derived in the present work receive the same improvements. The baseline aircraft shares most of the assumptions and calibration factors for various aspects of the aircraft design with the reference aircraft. The main flight controls of the Do228NG are mechanically operated, only the aileron trim and the stabilizer trim are electrically operated by the DC network [10]. A similar flight control system is assumed for the baseline and the silent commuter designs. The environmental control system (ECS) and the icing protection system, on the other hand, are fully electrified. Additional mass for heating and cooling equipment of the electric ECS is considered with 85 kg. The mechanical offtakes for an all-electric ECS are increased. The engine driven generator on the Do228NG puts out a nominal power of 6 kW [10]. For the designs of this study, a constant electrical offtake power of 18 kW is assumed to supply all aircraft power loads including the ECS. This rough estimate is considered as the maximum air conditioning setting on a regular mission. Although improvements in furnishing and operator items masses are expected, both are kept constant due to assumed increased comfort standards.

Table 3: Changes and improvements of baseline aircraft structures and propulsion system relative to the reference aircraft

Parameter		**Change**	**Rationale**
Masses	Wing	-15 %	Switch to CFRP structure
	Fuselage	-15 %	Switch to CFRP structure
	Empennage	-15 %	Switch to CFRP structure
	Gas turbine	-10 %	Material improvements and 3D-printing
	Nacelle	-10 %	Greater share of CFRP structure and improved production methods
Aerodynamics	Total drag	-5 %	Improved overall aerodynamic design
Geometry	Wing aspect ratio	From 9 to 11	Greater flexibility with CFRP material
Engine	Gas turbine efficiency	+15 %	Continuous improvement in gas turbine technology since the introduction of the engine of the reference aircraft in 1988.
	Technology	Bleedless	Better comparison with bleedless battery-electric aircraft
Maximum Payload		-40 kg	Reduced payload to increase battery mass budget

3.4 Hybrid Electric Architectures

Clean-sheet aircraft designs with hybrid-electric propulsion architectures and retrofits of existing designs have been reviewed and assessed extensively for CS23 and regional turboprop aircraft class [14, 15, 16, 17, 18, 19]. Two architectures are of particular interest to most of these studies: Parallel-hybrid (PHEP) and serial-hybrid electric (SHEP) propulsion systems. Both variants were modeled at the aircraft level and analyzed for their impact on noise emissions and energy efficiency. Functional principles, operational aspects and impacts on the aircraft modelling of the two architectures are briefly discussed hereafter. Figure 2 illustrates the basic principle of the two architectures.

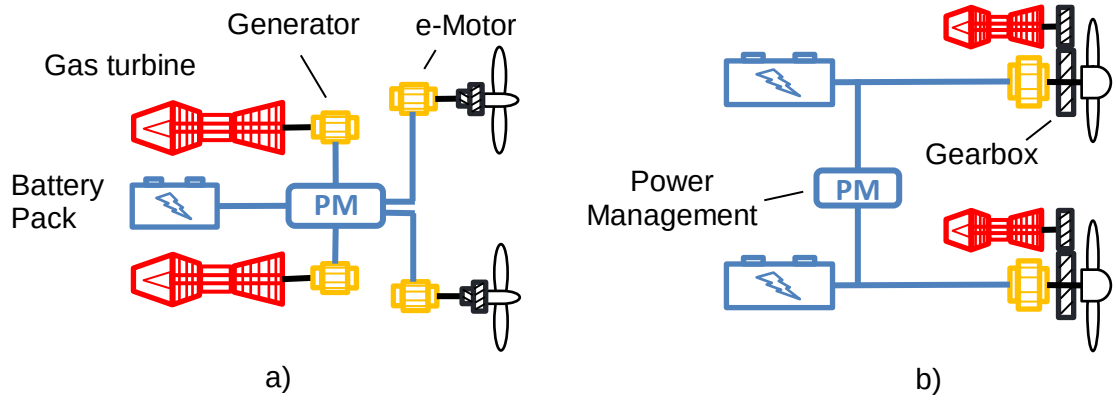

Figure 2: Basic principles of serial-hybrid a) and parallel-hybrid b) architectures

Parallel-Hybrid Architecture

In a PHEP architecture, an electric motor is mechanically coupled to the output shaft of a gas turbine. The coupling is either via a power combining gearbox (double-shaft parallel configuration) or the motor is mounted directly onto the gas turbine output shaft with, or without a transmission in front or behind the e-motor (single-shaft parallel configuration) [15]. This work addresses commuter aircraft, which typically employ turboprop engines that are classified as turboshaft engines. Turboshaft engines´ main output is shaft power with a small residual thrust power generated by the nozzle. Turboshaft engines of higher power classes typically employ free rotating power turbines that drive the propeller shaft through a gearbox. The PT6A-67D powering the Beechcraft 1900D is an example of such an engine [20], [21]. In the case of a hybrid aircraft with fully battery-electric flight capability it would be beneficial to include the option for mechanical decoupling of gas turbine from the e-motor. In this way, the gas turbine could be shut down when it is not needed, thus saving engine life and cost. For this purpose, a high-speed clutch that is built into a single-shaft parallel configuration is considered. Fitz et. al. [22] developed and tested a high-speed light-weight over-run clutch for rotorcraft applications with up to 20000 rpm and 5000 hp. For the purpose of the present work it is assumed, that similar clutches could be designed for aircraft applications. In this study the PHEP architecture is modelled for an aircraft with a conventional layout of 2 engines. A factor of 10 % extra mass is applied to the estimated gas turbine mass in the present aircraft engine model.

Serial-Hybrid Architecture

The shaft power of a gas turbine in a SHEP architecture is converted into electrical power via a generator and then transferred to an electric motor via a power management and distribution system. The motor drives a propulsor thereby generating thrust power. Multiple conversion of power imposes losses that puts the SHEP architecture at a disadvantage compared to the SHEP architecture. The mechanical decoupling of gas turbines and propulsors on the other hand gives the freedom to integrate both devices independently from each other. Furthermore, multiple propulsors per gas turbine are possible. For the SHEP aircraft model it was decided to choose four large propellers as thrust providers. The propeller wake and its interaction with the wing i.e. the impact on overall lift and drag is not considered for this study.

The CS-23 regulation makes no difference between two or four-engine airplanes with regard to take-off and minimum climb performance requirements [23]. The increased redundancy in thrust providers in the SHEP concept therefore makes it possible to downsize the engines according to other, less demanding operating points. This saves engine mass and increases the mass budget for the batteries and thus extends the range of the aircraft. The regulation is therefore advantageous for aircraft with higher propeller numbers.

3.5 Energy and Power Hybridization Scheme

Hepperle [24] has shown that to the first order the battery-electric range is proportional to the battery mass fraction. Practical battery mass fractions lie between 10 to 40 % total aircraft mass [24]. In order to achieve the maximum electric range with the silent commuter concepts, the MTOM limit of 8618 kg imposed by the CS-23 regulation is selected to serve as the target MTOM. The parametric studies of

the present work that were constrained by this target have resulted in battery mass fractions below 20 % and are thus compliant to the aforementioned limits. An advantage of this sizing strategy is that the batteries are of sufficient size to cope with the high take-off power requirements. Hence, fully battery-electric and local emission free flight can be accomplished. This flexibility in operation comes with a higher weight in electrical machines as they have to be also sized for the take-off power requirements. The gas turbines on the other hand can be downsized to maximum cruise conditions. They are only switched on to serve as range extenders and for the reserve mission. The derived energy storage sizing strategy and the power hybridization scheme was used on both the SHEP and the PHEP aircraft models.

3.6 Electric Power Components Modelling

3.6.1 Battery System

The results derived in the present work are tied to set of assumptions concerning the components of the hybrid-electric propulsion system. The underlying assumption for most of the electric components is a year of entry into service of 2030. The assumptions for the battery system are derived from target values agreed on in the Strategic Research Agenda formulated by the European Technology and Innovation Platform on Batteries - Batteries Europe consortium [25]. The reference provides roadmaps of the performance expectations of the battery technologies for the different mobility sectors. High energy aircraft batteries with a size of 250 to 1000 kWh are expected to exhibit a gravimetric energy density 500 to 600 Wh/kg on cell level at a discharge rate of 2C [25]. The more conservative lower limit of 500 Wh/kg was selected for the present work. The ratio of cell to battery pack mass for the same type of batteries is stated to be 80 to 90 % [25]. The lower limit of 80 % was selected. The resulting energy density on pack level is 400 Wh/kg. A 5 % mass penalty is assumed to consider structural integration in the airframe.

The volumetric energy density of high energy aircraft batteries has not been assessed in the Strategic Research Agenda [25]. The volumetric energy density is generally not a show stopper for battery-electric aircraft concepts, even if it can be rather critical for road vehicles. For light-duty road vehicles with battery sizes of 40 to 120 kWh a volumetric energy density of 1000 Wh/l is expected [25]. For the same batteries a cell-to-pack volume ratio of 75 % is formulated [25]. Due to an optimization on high gravimetric energy density the volumetric energy density for aircraft batteries might fare worse compared to batteries for road vehicles. A penalty of 5 % volume ratio is assumed, giving a battery pack usable volumetric energy density of 700 Wh/l for the present work. The allowable battery state-of-charge range on a standard mission is set between bounds of 90-20 % for this study. The discharge protection at lower limit is in line with other aircraft design studies based on lithium-ion batteries [18], [26]. The upper limit is a margin for battery degradation over the typical lifetime of the battery [18]. The combined charge/discharge cycle of the battery is assumed with an efficiency of 90 % [27]. Accounting for this efficiency gives the gross energy that has to be drawn from the grid to provide the assumed onboard usable battery energy for the mission. The cycle efficiency does not influence the sizing of the battery pack, as the provided battery pack characteristics are based on the energy and power output.

Table 4: Assumptions for installed batteries (timeframe 2030)

Parameter	Value	Unit
Battery cell specific energy	500	Wh/kg
Battery cell/pack weight ratio	80	%
Battery pack usable gravimetric energy density	400	Wh/kg
Battery cell usable energy density	1000	Wh/l
Battery cell/pack volume ratio	75	%
Battery pack usable energy density	700	Wh/l
State-of-Charge range for the main mission	90-20	%

3.6.2 Electric Motor, Power Converters & Thermal Management

The masses of electric motors and all other power converters except the cabling are estimated based on fixed power-to-mass ratios as is it is common on conceptual aircraft design level. The same holds

true for the component efficiencies which are assumed independent of the power load. High-speed, high power-to-mass permanent magnet electric machines have been modelled in disciplinary subdomains on a 2035 technology level [28]. According to the source, a power to mass ratio of 13.6 kW/kg for a high-speed gas turbine driven generator in the 2MW class was found to be feasible. Earlier works of Yoon et. al. [29] have shown the potential for power-to-mass ratios of more than 13 kW/kg for aircraft applications with efficiencies greater than 96 %. Based on these figures a power-to-mass ratio of 13 kW/kg was assumed for both the generator and for the e-motor in the propulsion chain. The various e-motor topologies modelled in [28] showed a plateau of the efficiency at about 97 %. This figure is selected for the present work´s e-motor and generator efficiency value.

A range of topologies, grid voltages and their influence on inverter mass was modelled in [28]. An average of 50 kW/kg was calculated from the spread given in [28] and is selected for the present work. The same power-to-mass ratio was assumed for the rectifier unit in the present work. The masses of power cables, circuit breakers and other electrical wiring, necessary for the propulsion chain, are summarized in a simple mass budget. This mass budget is difficult to assess on a conceptual level and represents one of the greater uncertainties in the design. It was assumed to be 50 kg for the parallel and 100 kg for the serial-hybrid due to increased cable lengths. The efficiency of the inverter and the rectifier was assumed to be 99 % and the efficiency of the transmission to be 99.5 %. Both the parallel and the serial-hybrid employ a two-stage gearbox between propeller and e-motor/gas turbine shaft. The gear ratio is assumed to be greater than 20 in order to allow high-speeds for the e-motor and the free power turbine. For the gearbox, a power-to-mass ratio of 12.5 kW/kg and an efficiency of 98.5 % are assumed. The turboelectric chain between generator and propeller shaft yields a total efficiency of 90.38 %. This value is significantly lower than the results from [28] (minimum 93 %) and is therefore considered valid for the 2030 timeframe. The thermal management equipment mass required for cooling of the power electronics is assumed to weigh 2 kW/kg [30].

Table 5: Assumptions for gear box, turboelectric chain and thermal management (timeframe 2030)

Parameter	Value	Unit
Gearbox, power density at gear ratio > 20	12.5	kW/kg
Gearbox, efficiency at gear ratio > 20	98.5	%
E-motor/Generator, power density at maximum continuous power	13	kW/kg
E-motor/Generator, efficiency at maximum continuous power	97	%
Inverter, power-to-mass ratio	50	kW/kg
Inverter, efficiency at maximum continuous power	99	%
Transmission efficiency	99.5	%
AC/DC Rectifier, power-to-mass ratio	50	kW/kg
AC/DC Rectifier, efficiency	99	%
Turboelectric chain serial-hybrid, efficiency	90.38	%
Heat load per kilogram of thermal management mass	2	kW/kg

3.7 Aircraft Configuration Aspects and Battery System Integration

The concept aircraft are designed to integrate the batteries inside the engine nacelles. The advantage is the good maintainability, safety and close proximity to the electric motors, which allows a minimum mass of electrical power distribution. In the SHEP concept, the mass of the combined propulsion and battery system is distributed evenly between the inner and outer nacelles, reducing the structural mass of the wing. The single nacelle on each side of the wing in the PHEP variant holds half of the battery packs. Consequently, it has a larger diameter and length compared to the inner nacelle in the SHEP concept.

The landing load case could be a problem with a body landing gear type as installed on the reference aircraft. Heavy reinforcements of the fuselage frame and wing structure may be required to bear the increased loads due to the battery nacelle integration. Therefore, the main landing gear is integrated into to the rear of the engine nacelles. This affects the high-lift system as the nacelles become long enough to disturb the flap retraction mechanism. The flapped trailing edge is interrupted by the elongated nacelle. This is a typical design known from other high-wing turboprop airliners such as the Fokker F-27 and the De Havilland DHC-8. The missing flapped area and thus high-lift capability is

partially recovered by the expansion of the outboard flaps from 60 to 65 % wing span.

3.8 Aircraft Systems

The all-electric ECS of the silent commuter concepts is either powered by the batteries, or a gas turbine driven generator in the PHEP concept, or the main generator in the SHEP concept. The propeller in the PHEP concept and thus the free power turbine can be stopped by a hydraulic brake in order to run one of the two gas turbines, thereby charging the batteries through the engine-driven generator. This enables autonomy on remote airfields where there is no suitable infrastructure to charge the batteries. In the SHEP design, this charging can be done more quickly because the gas turbine drives the main generator directly via the free power turbine at a higher power level.

3.9 Design for Noise Reduction

The objective of this paper is to design an electric commuter aircraft that is significantly quieter than existing 19-seater aircraft. However, there is no specific target for the noise level that must be achieved. Special regulation for 24/7 operation on German airfields with more than 15000 departures per year commands lower maximum noise levels than the ICAO standards [31]. The Do228NG that the reference aircraft is based on is already able to fulfill these requirements. To the knowledge of the authors there are no other more severe noise limits for commercial flight in Germany. For the current study, the target was set to achieve half the loudness compared to the reference aircraft. This is expressed in a reduction of 10 dB(A). This delta in A-weighted sound pressure level (SPL) is commonly known to result in half the perceived noise for a human and represents a comprehensible target for the study at hand. In the following, two noise reduction strategies are discussed.

3.9.1 Take-off and Landing Performance

From the initial discussions on what a battery-electric commuter concept could look like, it was found that short take-off and landing capabilities could facilitate the success of such an aircraft. These capabilities fall in line with the ability to reduce noise emissions. The DHC-7 STOL airliner, for instance, creates a much smaller noise footprint area compared to conventional take-off and landing (CTOL) turbofan aircraft of its era [32]. This is in part enabled by steep approach angles of 7.5° instead of the regular 3° approach and by the short take-off field length. Therefore, an optimized take-off performance for the silent commuter concepts of the present study was sought. According to Roskam [33], the minimum take-off power for a required take-off field length is inversely proportional to the maximum achievable lift coefficient. Furthermore, lower take-off power generates less noise as confirmed by parametric studies on the PHEP concept. The reduction in take-off power yields a smaller propulsion chain mass, thus adding mass budget to the battery system. A possible design trade-off would be to vary the lift coefficient until a global performance optimum is found. At first, the take-off field length requirement is sizing for the propeller shaft power but at some point, along the trade-off it is superseded by other power requirements, for instance the climb requirement in one-engine inoperative case or the top-of-climb power requirement. The approach speed is lowered from 85.5 KCAS (reference aircraft) to 80 KCAS in order to meet the shorter landing field requirement.

3.9.2 Propeller Design

The dominant noise source during take-off proved to be the propeller [8]. Hence, the optimization of this component is critical to the overall noise reduction of the concept aircraft. The same noise estimation method from Froehler [8] is applied in the present study. A starting point for the propeller design is the propeller of the reference aircraft. As shown in Table 2, the Dornier 228NG features a five bladed propeller with a diameter of 2.5 m and a maximum rotational speed of 1591 rpm. The maximum shaft power of the propeller is 580 kW. The calibrated low-speed and high-speed propeller performance models are used for the baseline and conceptual aircraft calculations.

The high-speed propeller performance model is of low level of fidelity with sensitivities on the number of propeller blades and on the propeller disk loading. The propellers are always assumed to be operated at optimal speeds during the mission. The model is used for the aircraft mission calculation. The low-speed propeller performance model, which is used for the take-off calculations, is also sensitive on the propeller disk loading and blade number. However, the rotational speed is dependent on the propeller shaft power, thrust and blade count. The simplified model considers a constant blade activity factor for all possible configurations of blade number and diameter. The activity factor is related to the

amount of power that a propeller blade can absorb [34].

The propeller diameter and blade number were varied in an overall aircraft design parametric study in order to derive the trade-off between the overall aircraft performance and noise emissions, which will be described more in detail in the following section.

4. Noise Assessment

4.1 ICAO Take-off Reference Procedure

The ICAO has published recommendations, but no mandatory noise limit regulations for aircraft with STOL capabilities [35]. The focus of this study is to produce comparable results. Hence, the ICAO noise limits and measurement procedure according to Annex 16, chapter 10 for propeller-driven aircraft not exceeding 8618 kg MTOM was selected. The critical metric is the maximum A-weighted sound pressure level (SPL) measured on the centerline of the trajectory from an observer 2500 m away from brake-release point [35]. This metric is calculated for the conceptual aircraft design model used in this study with the method introduced in [8]. Further procedural instructions are that the engine setting has to be take-off power the entire take-off phase and the aircraft has to accelerate to its best rate-of-climb speed V_y at the high-lift configuration that is considered normal for the climb segment [35]. In the present study the latter was considered to be the clean, flaps-up configuration. The altitude of the take-off segment where the flaps are retracted and the aircraft accelerates to V_y was set to constant 400 ft above ground level for all aircraft designs. Each calculated aircraft accelerates to its individual V_y.

The certified noise level at take-off of the Do228NG with the five-blade propeller installation is 76.7 dB(A) [36]. The calculation of the reference aircraft resulted in a value of 75.8 dB(A), which is in sufficient agreement with the official data.

4.2 Parametric Study

A parametric study was carried out in order to assess the concept aircraft with regard to noise emission depending on changes in take-off lift coefficient, propeller diameter and blade number. In the subsequent paragraphs, results of these trade-offs are shown and candidate configurations for the PHEP and SHEP concepts identified.

4.2.1 Influence of Take-off Power

In the conceptual aircraft models, the take-off lift coefficient is controlled via the flap deflection angle. The intended trade-off between lift coefficient, take-off power, noise and battery-electric range was detailed in paragraph 3.9.1. The range was calculated for each sample with maximum cruise speed. Figure 3 shows the change in A-weighted SPL, lift coefficient, installed propeller shaft power at each engine and range for the PHEP concept. A reduction in SPL is observed for higher flap deflection angles.

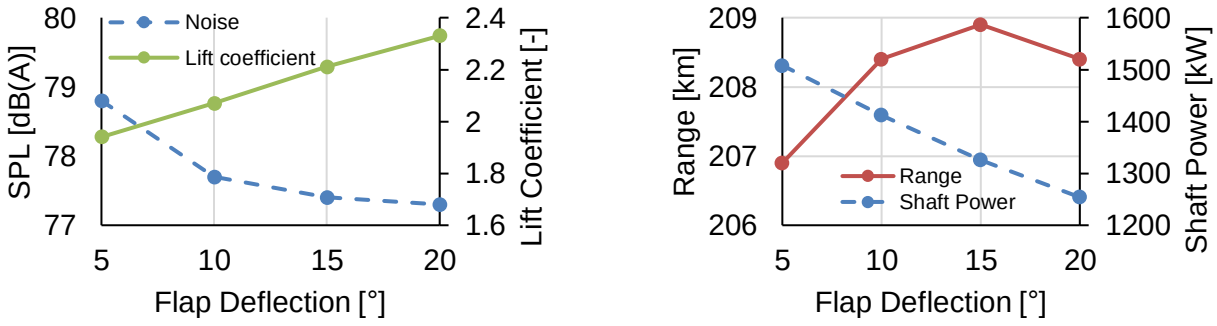

a) b)

Figure 3: Influence of flap setting on a) lift coefficient and A-weighted SPL
b) total shaft power and range for the PHEP concept

At the same time, the installed shaft power is reduced by more than 16%, providing more mass budget for the battery system. However, the range shows a plateau at a flap deflection of 15°. Increasing the

flap angle decreases the take-off speed, which reduces the effectiveness of the vertical tail plane (VTP). Therefore, the VTP size is increased, which reduces the total lift-to-drag ratio and the range. This negative effect offsets the higher mass budget for the battery system. Because of these results, a flap deflection angle of 15° is considered optimal and is chosen for both PHEP and SHEP concepts for all designs.

4.2.2 PHEP Case

The variation of blade number was done on the PHEP concept, varying from five to seven bladed propellers for diameters between 2.5 and 3.0 m. An important boundary condition for the trade is the assumed constant activity factor for the propeller blades (see paragraph 3.9.2). This means that the maximum thrust capability depends on the propeller diameter, the number of blades and the rotational velocity of the propeller. Increasing the number of blades allows the propeller to provide the needed thrust at lower rotational speed, as the loading per blade is lower. Moreover, the noise frequency spectrum is shifted favorably towards higher frequencies, resulting in overall noise reduction. However, there are negative effects on the aircraft performance. The propeller efficiency in cruise decreases with more propeller blades due to the constant activity factor assumption. Furthermore, the propeller mass increases, which reduces the available mass budget for the battery. The performance penalty is quantified in terms of electric range decrease. Figure 4 a) and b) show the reduction in total required shaft power and rotational speed, respectively, with increasing propeller diameter and blade number. The installed propeller shaft power is sized by the take-off field length requirement in all cases. Increasing the blade number requires slightly more propeller shaft power due to the higher drag penalty when the inoperative propeller is feathered at take-off. The results show that a 3.0 m diameter propeller requires about 11 % less shaft power compared to a 2.5 m diameter propeller. Furthermore, the rotational speed drops by 24 %.

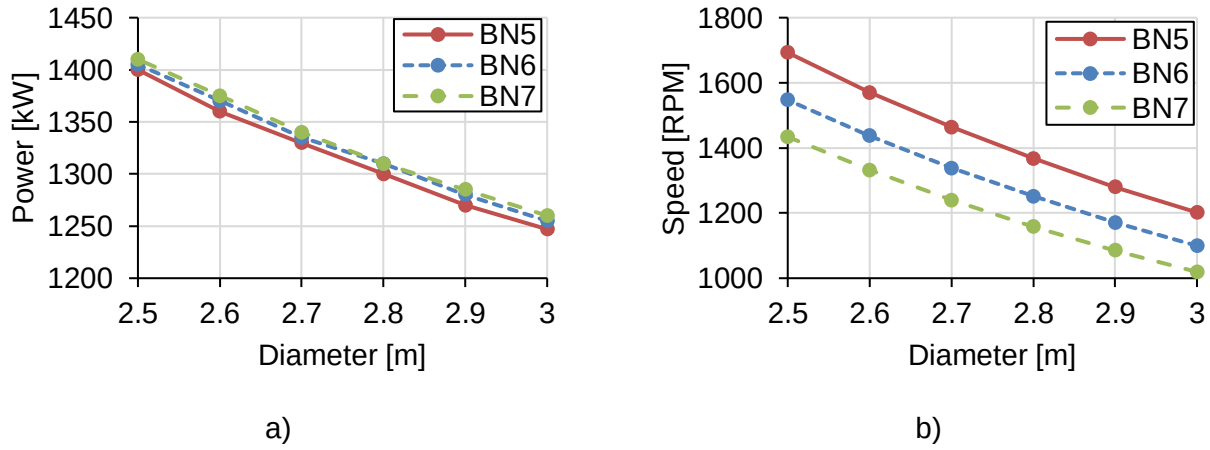

Figure 4: Influence of diameter and number of blades on a) total required propeller shaft power, b) propeller speed for the PHEP concept

Figure 5 a) shows the change in A-weighted SPL dependent on the propeller diameter and blade number. A reduction of propeller noise is observed with increasing blade number and diameter. This is caused by the lower rotational speeds and the reduced power loading. One exception is observed for the 2.5 m diameter props: The propeller with five blades is quieter than the six-blade design. This is due to the discrete nature of the A-weighting in the frequency analysis which happens to compliment the specific blade pass frequency of the five-blade configuration. The seven-blade propellers yield the lowest noise levels. However, with increasing diameter the benefit to six-blade designs diminishes and ceases at a diameter of 3.0 m. None of the configurations fulfill the target noise level reduction of 10dB(A) to the reference aircraft.

Figure 5 b) shows the change in battery-electric range dependent on the diameter and blade number. On average, the five blade designs yield 2.9 % higher performance compared to the seven-blade designs. Between 2.5 m and 2.8 m diameter a continuous improvement in range is observed for all blade numbers. From 2.8 m upwards, the range grows slower or remains constant in case of the seven-blade design. Larger diameters increase the propeller mass and thus reduce the mass budget for the battery pack. Furthermore, bigger propellers need to be installed at a more outward spanwise

position to ensure sufficient clearance to the fuselage. This results in a larger one engine inoperative yaw moment due to the longer lever arm, ultimately resulting in a bigger VTP, affecting both the structural mass and the aircraft drag. Larger propeller diameters also require slower rotational speeds i.e. higher gear ratios in case the gas turbine output speed is constrained. The applied gear box mass estimation method is sensitive to shaft power, but not to gear ratio. Therefore, the range is expected to be further penalized for bigger diameters.

The six-blade, 3.0 m diameter propeller configuration is selected for the PHEP concept. It yields the lowest noise level with better efficiency and less complexity compared to the seven-blade designs.

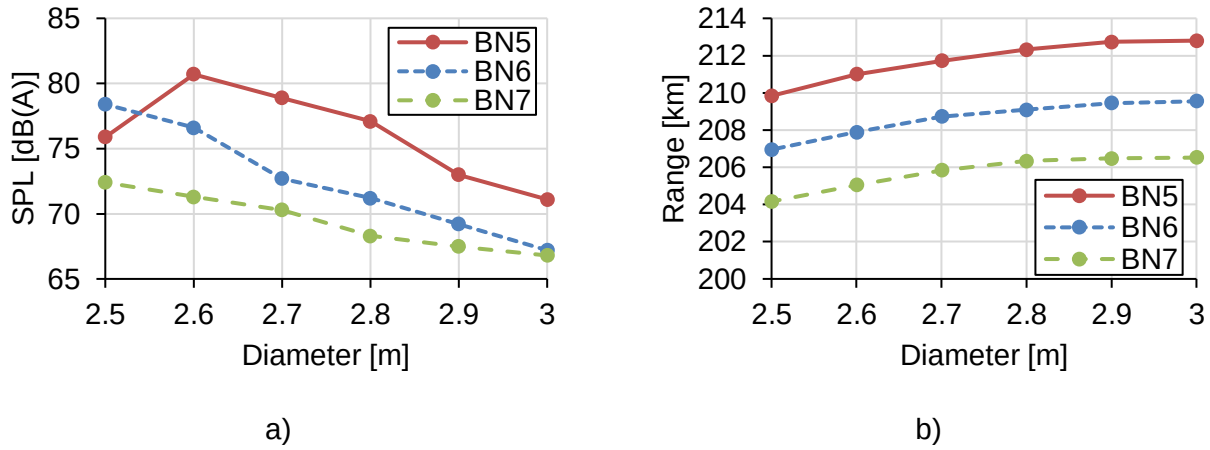

Figure 5: Influence of diameter and number of blades on a) maximum A-weighted SPL, b) battery-electric range with maximum speed for the PHEP concept

4.2.3 SHEP Case

In the study for the SHEP concept, the variations were done between three and four blades per propeller and for diameters between 2.5 and 2.8 m. The same principles as described in paragraph 4.2.2 apply to this trade-off. Figure 6 a) and b) show the total required shaft power and rotational speed of each propeller, respectively, as a function of diameter and the number of blades. The required shaft power is reduced by as much as 27% compared to a PHEP configuration with the same propeller diameter. In general, for the SHEP cases, the required shaft power showed to be almost independent of the propeller diameter. All of the designs are sized by the maximum cruise operating point.

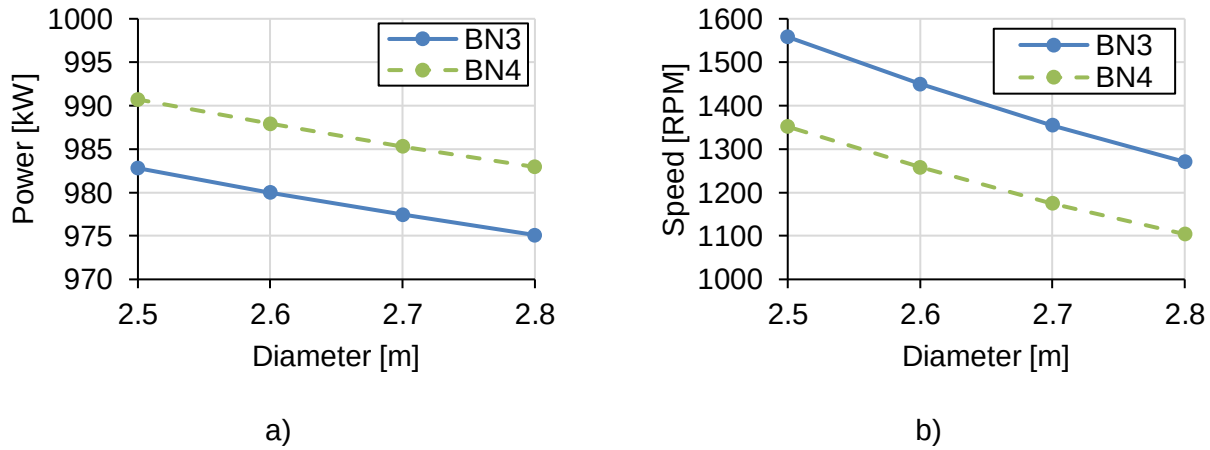

Figure 6: Influence of diameter and number of blades on a) required total shaft power, b) propeller speed for the SHEP concept

The lower shaft power for larger diameters results from the increased propeller efficiency in cruise. As a result, the available shaft power is oversized at take-off. Similar to the PHEP case, the propeller rotational speeds drop with increasing diameter.

Figure 7 a) shows the change in A-weighted SPL dependent on the propeller diameter and blade

number. The four-blade design´s noise levels remain below those of the three-blade design´s for all analyzed diameters. Furthermore, all four-blade designs fulfill the target noise reduction of -10 dB(A) compared to the reference aircraft. Only the 2.7 m and 2.8 m diameter three-blade propellers fulfill the target. The largest gradients in SPL reduction can be observed between diameters of 2.5 and 2.7 m for the three-blade designs and between 2.5 and 2.6 m for the four-blade designs. Diameters greater than 2.6 m show no significant benefit in noise reduction for the four-blade design.

Figure 7 b) shows the change in battery-electric range dependent on the diameter and blade number. Overall, the three-blade designs perform 2 % better compared to the four-blade designs. The changes in propeller shaft power across the range of analyzed diameters is small for both the three-blade and four-blade configurations. Thus, any increase in propeller efficiency due to greater diameters is compensated by higher propeller masses. The propeller diameter influence on range is therefore considered negligible. The propellers in the SHEP concept are solely driven by electric motors. The gear ratio of the gearbox connecting the two components and the e-motor speed can be freely optimized to achieve the lowest total mass. This is an advantage compared to the PHEP concept, where the gas turbine output speed might constrain the drivetrain.

The three-blade design with 2.7m diameter is the smallest propeller to achieve the required noise reduction and thus is selected for the SHEP concept. Furthermore, it performs better in terms of range than the four-blade design. Smaller diameters are preferred in general, since they provide better ground clearance and might reduce propeller cost.

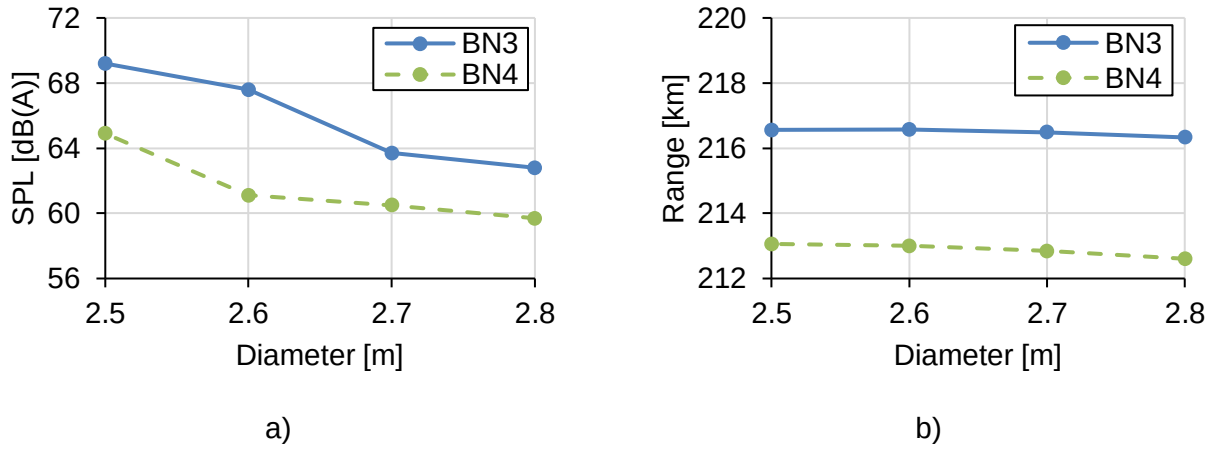

Figure 7: Influence of diameter and number of blades on a) maximum A-weighted SPL, b) battery-electric range with maximum speed for the SHEP concept

4.2.4 Selection and Discussion of Final Designs

Increasing the blade number and decreasing the rotational speed showed to have a positive influence on aircraft noise level. Also, increasing the blade number allows further reduction of the rotational speed without degrading the thrust characteristics of the propeller. However, increasing the propeller blade number comes with the cost of reducing the high-speed performance of the aircraft. Increasing the propeller diameter is another degree of freedom in the design space. It allows for decreasing the rotational speed without degrading the thrust capabilities of the propeller, which is similar to increasing the blade number. Furthermore, the cruise efficiency of the propeller tends to improve for bigger diameters. However, the increasing propeller mass diminishes this positive effect. There is another significant performance penalty specific to twin turboprop configurations: bigger propellers require greater VTP sizes due to the increased one engine inoperative yaw moment (see paragraph 4.2.2) However, the diameter trade-off is less performance-sensitive for the SHEP configuration, as the increased redundancy relaxes the VTP sizing constraints. For this reason, the four-propeller design optimization results in significantly bigger total disk area with less blades per propeller.

Two promising configurations for the PHEP and the SHEP concept were then selected and compared to the reference aircraft. The final PHEP concept features six-blade propellers and a diameter of 3.0 m. The final configuration of the SHEP concept features three-blade, 2.7 m diameter propellers. Figure 8 shows the take-off trajectories of reference, and the final PHEP and SHEP aircraft models and the observer position at 2500 m distance from break release point. The SHEP concept´s V_y and maximum rate-of-climb are lower compared to the other aircraft, which is why it climbs earlier and slower. This

enables a greater distance to the observer at all positions along the trajectory, hence, reducing the noise level.

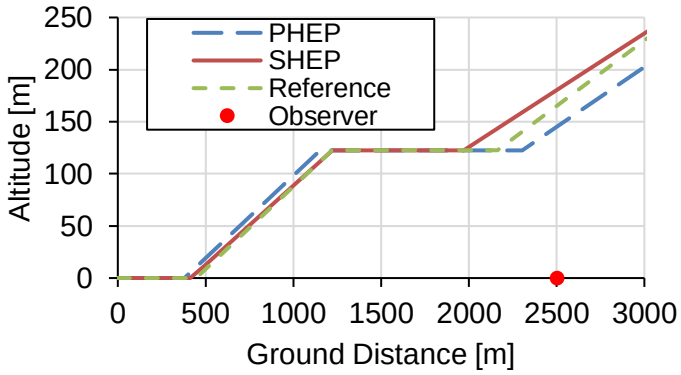

a)

Metric	PHEP	SHEP	Ref.
SPL [dB(A)]	67.2	63.7	75.8
V_y [KTAS]	135.3	115.5	135.3
maxROC [ft/min]	1608	1267	1713

b)

Figure 8: a) Take-off trajectories, b) best rate-of-climb speeds and maximum rate-of-climb at MTOM, SL ISA conditions for SHEP, PHEP and the reference aircraft

The selected PHEP concept shows 8.6 dB(A) noise level reduction compared to the reference aircraft. This result is close to the target reduction of 10 dB(A) set for the study. Moreover, a similar reduction can be expected if the baseline aircraft were to be redesigned in a similar manner. This result is interesting, as it shows that a significant noise reduction can be achieved also for conventional twin configuration through a dedicated propeller design. The final SHEP concept achieves a 12.1 dB(A) reduction in SPL, mainly due to the significant increase in propeller disk area, and lower required take-off power. This result shows that distributed propulsion concepts can be a good choice for challenging noise reduction targets.

5. Design Results

One candidate propeller configuration for each propulsion architecture was selected as final design. Figure 9 a) shows an axonometric view of the selected SHEP concept and Figure 9 b) the PHEP variant. Both designs are compared with the baseline aircraft with regard to aircraft geometry and performance (Table 6).

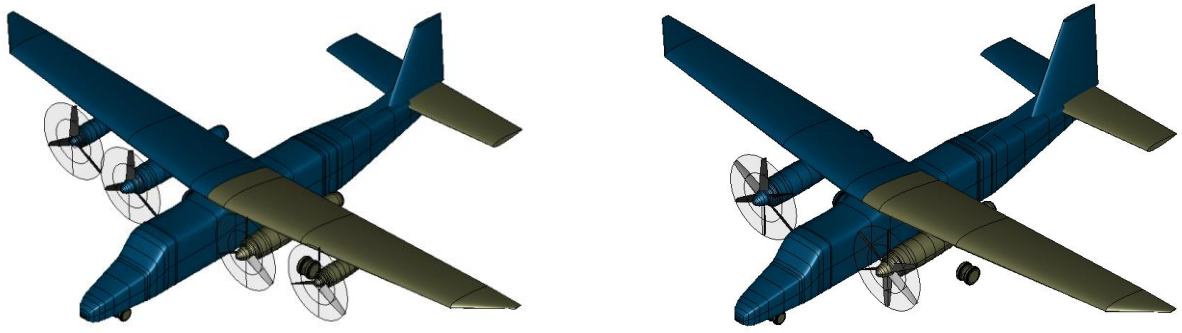

a) b)

Figure 9: Axonometric view on final SHEP concept in a) and final PHEP concept in b)

The main differences between the silent electric commuter concepts and the baseline aircraft are the bigger wing, the nacelle-mounted landing gear and the higher maximum lift-to-drag ratio. The increased lift-to-drag ratio is due to the greater wing area. It causes a reduction in non-dimensional drag of components such as the fuselage, the empennage and the engine nacelles. The relaxed requirements in one engine-inoperative conditions due to increased redundancy allow the total shaft power in the SHEP concept to be downsized to the level required for maximum cruise speed.

Table 6: Geometrical and performance data of hybrid-electric concept and baseline aircraft

Item	Unit	PHEP	SHEP	Baseline
Geometry				
Wing area	m^2	48.7	48.5	32.1
Wing aspect ratio	-	11	11	11
Wing span	m	23.1	23.1	18.8
VTP area	m^2	7.5	5.3	6.0
VTP aspect ratio	-	1.4	1.4	1.4
HTP area	m^2	12.0	11.9	7.4
HTP aspect ratio	-	4.8	4.8	5.2
Performance				
L/D, max. cruise	-	12.21	12.23	10.90
L/D, max	-	20.53	20.54	18.84
Power				
Shaft power, installed, SL ISA	kW	1256	977	960
Battery power, 2C discharge	kW	1408	1399	0

Table 7 lists the overall mass breakdown for each aircraft concept. The PHEP variant benefits from a 3.3 % lower propulsion mass compared to the SHEP variant. The SHEP concept partially compensates this with its smaller VTP area and therefore lower structural mass. However, the PHEP configuration, requires less reserve fuel and thus can load more battery mass.

Table 7: Mass breakdown of hybrid-electric concept and baseline aircraft

Item	Unit	PHEP	SHEP	Baseline
Structure	kg	2008	1976	1582
Propulsion	kg	1072	1109	545
Battery, installed	kg	1848	1836	0
Systems	kg	745	745	745
Furnishings	kg	270	270	270
Manufacturer empty mass (MEM)	kg	5943	5936	3142
Operating items	kg	475	475	475
Operating empty mass (OEM)	kg	6418	6411	3617
Maximum payload	kg	2000	2000	2000
Maximum zero fuel mass (MZFM)	kg	8418	8411	5617
Maximum landing mass (MLM)	kg	8617	8618	5749
Maximum take-off mass (MTOM)	kg	8617	8618	5993

Table 8 shows the breakdown for the propulsion chain for the two silent electric designs and the baseline aircraft. The SHEP concept profits from the lower take-off power requirement due to the lower relative thrust loss in case that one engine fails. This results in a lower gearbox, e-motor and gas turbine mass.

Table 8: Mass breakdown of propulsion chains for silent commuter concepts and baseline aircraft

Item	Unit	PHEP	SHEP	Baseline
Propellers	kg	212	174	140
Gearboxes	kg	113	78	87
E-Motors	kg	98	76	0
Inverters	kg	26	20	0
Cabling	kg	50	100	0
Cooling	kg	36	52	0

Item	Unit	PHEP	SHEP	Baseline
Rectifiers	kg	0	21	0
Generators	kg	0	81	0
Clutches	kg	21	0	
Gas turbines	kg	206	217	183
Gas turbine mount structures	kg	43	38	27
Engine systems	kg	76	65	60
Nacelles	kg	191	187	49
Propulsion	kg	1072	1109	1084

The payload range characteristic for long range speed is shown in Figure 10. Long range operation means cruising at high lift-to-drag ratio but a slow speed of 140 KTAS. The SHEP concept achieves 6.5 % greater battery-electric range than the PHEP concept. This is due to the SHEP concept´s higher propeller efficiency and smaller VTP size. The ferry range of the SHEP concept is about 2.1 % lower compared to the ferry range of the PHEP concept. Again, the SHEP concept´s higher propeller efficiency and a slightly higher lift-to-drag ratio compensate in part for the conversion losses in the power train. Therefore, the SHEP architecture can compete on all ranges. The baseline model surpasses both hybrid-electric concepts with a greater range utilization for all payloads but close to the ferry range. The bigger wings of the hybrid-electric models leave room for greater fuel tanks.

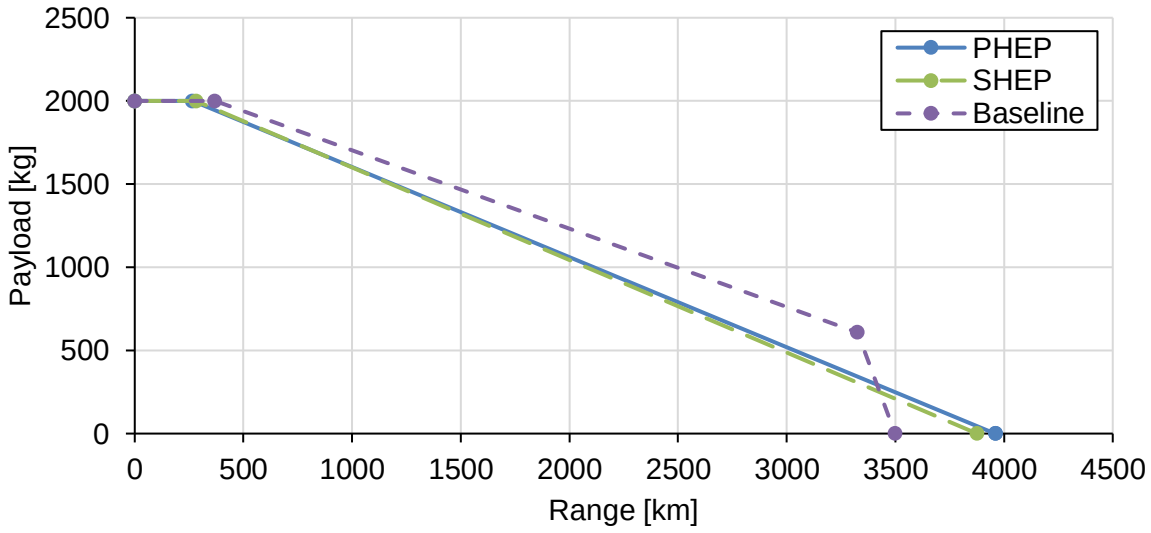

Figure 10: Payload range comparison between serial-hybrid, parallel-hybrid and baseline aircraft for long range speed

All concepts are evaluated on two statistical relevant distances with a standard passenger payload. More than half of the 19-seater world fleet missions in the year 2018 served a stage length of up to 200 km [2]. Moreover, 77 % of the twin-turboprop stage lengths flown in the year 2017 within, from and to the US ranged up to 400 km [18]. Therefore, the block fuel and the block electric energy and the total energy demand for both of these distances are listed in Table 9. The energy demand of any of the hybrid-electric aircraft concepts is a fraction of the energy demand of the baseline aircraft. This follows from the fact that the conversion from battery-electric energy to shaft energy is much more efficient compared to the combustion of fuels. Furthermore, the SHEP concept saves 6.0 % energy compared to the PHEP concept on a stage length of 200 km and 7.1 % on a stage length of 400 km. Overall, the SHEP concept operates more efficiently in the low speed domain than the PHEP concept.

Table 9: Evaluation of block electric energy and block fuel demand for all hybrid-electric concepts and the baseline aircraft on a short haul mission with long range speed and SPP

Stage Length	Metric	Unit	PHEP	SHEP	Baseline
200 km	Block electric energy [kWh]	kWh	402	378	0
	Block fuel	kg	0	0	118

Stage Length	Metric	Unit	PHEP	SHEP	Baseline
200 km	Total energy	kWh	402	378	1417
400 km	Block electric energy	kWh	522	518	0
	Block fuel	kg	75	67	213
	Total energy	kWh	1422	1321	2557

6. Conclusion

Two plug-in hybrid aircraft concepts, one with a serial-hybrid (SHEP), the other with a parallel-hybrid-electric propulsion architecture (PHEP), were designed with an assumed 2030 technology status. The TLARs for the designs were derived from observing the latest trends in the 19-seater, commuter aircraft market. The short-haul, low-speed domain with flexible passenger and cargo transport capability was presumed to suit the strengths of battery-electric aircraft. Short take-off and landing capabilities as well as low-noise design targets were set as means for expanding the market potential. The concept of a fully electric flight capability combined with gas turbines serving as range extenders in cruise flight and for mission reserves was selected for both propulsion architectures. Parametric studies on relevant design characteristics of the propellers were carried out for the overall aircraft design optimization.

The results showed that the plug-in concepts can achieve all-electric operation on missions over 200 km, which is the median utilization distance of the commuter aircraft fleet. As shown in Table 9, the energy savings at this range are about 72 % compared to the conventional twin turboprop baseline concept with the same EIS used for the modelling. Furthermore, the range extender concept ensures that longer missions can also be served efficiently. Around 80 % of the current commuter traffic takes place under 400 km, where the plug-in concepts cut the block energy consumption by more than half.

Moreover, the SHEP configuration can potentially achieve more than 10 dB(A) reduction in maximum sound pressure level compared to the reference aircraft at take-off. This can be regarded as a 50 % reduction in perceived noise. Furthermore, this is achieved without degradation of the aircraft energy efficiency compared to a design without noise optimization boundary conditions. The main benefit of the serial-hybrid architecture is the energy and weight efficient augmentation of thrust capability of the aircraft through additional propulsors.

The PHEP configuration potentially offers slightly greater mission ranges (Figure 10) and even more so, when there are no noise-related boundary conditions. It showed no particular benefit in noise reduction compared to conventional designs. The final PHEP design with a low-noise propeller achieved a noise level reduction of about 8.6 dB(A) compared to the reference aircraft. However, this low-noise design took a higher toll in terms of performance than for the SHEP concept. As can be seen in Figure 8 b) and Table 9, the final SHEP design is not only quieter but also more energy efficient than the final PHEP configuration. The benefits of the PHEP architecture are the more conventional design with fewer components and a less complex system architecture, which helps to reduce time and costs for development and certification. However, the SHEP architecture, proved to be synergetic for designs with more challenging noise emissions constraints.

The focus of this paper was on the primary design drivers in hybrid-electric aircraft design. Fast and simplified methods were used to derive major sensitivities in propeller design, electric machines and electric power distribution. In order to improve the fidelity in the design process, the authors suggest to apply higher tier methodology, especially in the field of gearbox modelling, propeller performance and propeller wake-wing interaction.

7. Acknowledgments

The authors would like to thank Johannes Autenrieb for his support in vertical tail plane stability analysis.

8. Contact Author Email Address

Philip Wassink, German Aerospace Center, 22119 Hamburg, Germany

Mailto: philip.wassink@dlr.de

9. Copyright Statement

References

[1] European Commission, "Flightpath 2050 Europe's Vision for Aviation," European Union, Belgium, 2011.

[2] A. Paul, W. Grimme, G. Atanasov, J. van Wensveen and F. Peter, "Evaluation of the Market Potential and Technical Requirements for Thin-Haul Air Transport," in *Deutscher Luft- und Raumfahrtkongress*, 2019.

[3] G. Atanasov, J. van Wensveen, F. Peter und T. Zill, „Electric Commuter Transport Concept Enabled by Combustion Engine Range Extender," in *Deutscher Luft- und Raumfahrtkongress*, 2019.

[4] F. Salucci, L. Trainelli, M. Bruglieri, C. Riboldi, A. Rolando and G. G. González, "Capturing the Demand for an Electric-Powered Short-Haul Air Transportation Network," in *AIAA Scitech 2021 Forum*, Virtual Event, 2021.

[5] V. Papantoni, K. Dietl, J. Scherer and G. Bona, "Assessment of Three Commuter Aircraft Concepts from a Transport System Perspective," in *International Council of the Aeronautical Sciences*, Shanghai, 2020.

[6] S. Wöhler, G. Atanasov, D. Silberhorn, B. Fröhler and T. Zill, "Preliminary Aircraft Design within a Multidiciplinary and Multifidelity Design Environment," Aerospace Europe Conference 2020, Bordeaux, France, 2020.

[7] M. Alder, E. Moerland, J. Jepsen and B. Nagel, "Recent Advances in Establishing a Common Language for Aircraft Design with CPACS," in *Aerospace Europe Conference*, Bordeaux, 2020.

[8] B. Fröhler, G. Atanasov, C. Hesse and P. Wassink, "Disciplinary Sub-Process to Assess Low-Speed Performance and Noise Characteristics Within an Aircraft Design Environment," in *Deutscher Luft- und Raumfahrtkongress*, 2020.

[9] Textron Aviation Inc., "First Cessna SkyCourier twin utility turboprop takes flight," Wichita, 2020.

[10] RUAG Aerospace Services GmbH, "Pilot´s Operating Handbook Do228-212," 2009.

[11] RUAG Aerospace Services GmbH, "Dornier 228 Advanced Commuter (AC) Facts and Figures," 2019.

[12] National Business Aviation Association, "NBAA Management Guide," 2011.

[13] European Commission, "EU OPS Subpart D," 2008.

[14] D. F. Finger, C. Braun and C. Bil, "Comparative Assessment of Parallel-Hybrid-Electric Propulsion Systems for Four Different Aircraft," *Journal of Aircraft,* vol. 5, no. 57, September-October 2020.

[15] Y. Xie, A. Savvarisal, A. Tsourdos, D. Zhang and J. Gu, "Review of hybrid electric powered aircraft, its conceptual design and energy management methodologies," *Chines Journal of Aeronautics,* vol. 4, no. 34, pp. 432-450, April 2021.

[16] M. Strack, T. Zill and B. Nagel, "Integration of Hybrid Propulsion in a CS23 Commuter Design," in *Congress of the International Council of the Aeronautical Sciences*, Daejeon, 2016.

[17] P. Juretzko, M. Immer and J. Wildi, "Performance analysis of a hybrid-electric retrofit of a RUAG Dornier Do228NG," *CEAS Aeronautical Journal,* no. 11, pp. 263-275, 2020.

[18] I. Staak, A. Sobron and P. Krus, "The Whole Thruth About Electric-Powered Flight for Civil Transportation: From Breguet to Operational Aspects," in *Aerospace Europe Conference*, Bordeaux, 2020.

[19] S. Byahut and A. Uranga, "Propulsion Powertrain Component Modelling for an All-Electric

Aircraft Mission," in *AIAA Scitech Forum*, Orlando, 2020.

[20] Federal Aviation Administration, "Type Certificate Data Sheet No. A24CE," 1998.

[21] European Aviation Security Agency, "Type Certificate Data Sheet No. EASA.IM.E.008," 2019.

[22] F. Fitz and C. Gadd, "Design, Fabrication, and Testing of a High-Speed, Over-Running Clutch for Rotorcraft," 1998.

[23] European Aviation Safety Agency, „Certification Specifications and Acceptable Means of Compliance for Normal, Utility, Aerobatic and Commuter Category Airplanes CS-23," 2015.

[24] M. Hepperle, "Electric Flight - Potential and Limitations," 2012.

[25] European Technology and Innovation Platform on Batteries - Batteries Europe, "Strategic Research Agenda," European Commision, 2020.

[26] J. Hölzen, L. Yaolong, B. Bensmann, C. Winnefeld, A. Elham, J. Friedrichs and R. Hanke-Rauschenbach, "Conceptual Design of Operation Strategies for Hybrid Electric Aircraft," *Energies,* p. 217, 16 Januar 2018.

[27] U. Maier and M. Deutsch, "https://www.agoraverkehrswende.de/fileadmin/Projekte/2017/Die_Kosten_synthetischer_Brenn-_und_Kraftstoffe_bis_2050/Agora_SynCost_Webinar_slides_Deutsch_and_Maier_20180516.pdf," 2018. [Online]. [Accessed 5 Mai 2021].

[28] S. Biser, M. Filipenko, M. Boll, N. Kastner, G. Atanasov, M. Hepperle, D. Keller, D. Vechtel and M. Noe, "Design Space Exploration Study and Optimization of a Distributed Turbo-Electric Propulsion System for a Regional Passenger Aircraft," in *AIAA Propulsion and Energy Forum*, Virtual Event, 2020.

[29] A. Yoon, X. Yi, J. Martin, Y. Chen and K. Haran, "A high-speed, high-frequency, air-core PM machine for aircraft application," in *IEEE Power and Energy Conference*, Illinois, 2016.

[30] T. Spierling and C. Lents, "Parallel Hybrid Propulsion System for a Regional Turboprop: Conceptual Design and Benefits Analysis," in *AIAA Propulsion and Energy Forum*, Indianapolis, 2019.

[31] Luftfahrt-Bundesamt, "Übersicht Landeplatz-Lärmschutz-Verordnung vom 5. Januar 1999," 2004.

[32] F. Buller and A. Toplis, "The DHC-7, first generation transport category STOL - Particular design challenges," in *AIAA 4th Aircraft Design, Flight Test, and Operations Meeting*, Los Angeles, 1972.

[33] J. Roskam, Airplane Design Part I to VII, DARcorporation, 1985 - 1990.

[34] J. Roskam und C.-T. Lan, Airplane Aerodynamics and Performance, 1997.

[35] International Civial Aviation Organization, "Annex 16 to the Convention on International Civil Aviation," 2017.

[36] European Aviation Safety Agency, „Type Certificate Data Sheet for Noise No. A.359 - Dornier 228," 2016.

[37] I. Geiß and A. Strohmayer, "Operational Energy and Power Reserves for Hybrid-Electric and Electric Aircraft," in *Deutscher Luft- und Raumfahrtkongress*, 2020.

[38] P. Jackson, K. Munson and L. Peacock, "Jane´s all the world´s aircraft," Sentinel House, Surrey, 2002.

[39] Pornet, Kaiser, Isikveren and Hornung, "Integrated fuel-battery hybrid for a narrow-body sized transport aircraft," *Aircraft Engineering and Aerospace Technology,* vol. 6, no. 86, pp. 568-574, 2014.

[40] C. Pornet, Conceptual Design Methods for Sizing and Performance of Hybrid-Electric Transport Aircraft, München, 2018.

[41] A. Seitz, M. Nickl, A. Stroh and P. C. Vratny, "Conceptual study of a mechanically integrated parallel hybrid electric turbofan," *Journal of Aerospace Engineering,* vol. 12, no. 232, pp. 2688-2712, 2018.

[42] European Aviation Safety Agency, "Supplemental Type Certificate 10014953 REV. 3," 2020.